

## Supporting Information

### **Chemical and Structural Configuration of Pt Doped Metal Oxide Thin Films Prepared by Atomic Layer Deposition**

Ranjith K. Ramachandran,<sup>\*,†</sup> Matthias Filez,<sup>‡,⊥</sup> Eduardo Solano,<sup>†,∇</sup> Hilde Poelman,<sup>‡</sup> Matthias M. Minjauw,<sup>†</sup> Michiel Van Daele,<sup>†</sup> Ji-Yu Feng,<sup>†</sup> Andrea La Porta,<sup>||</sup> Thomas Altantzis,<sup>||</sup> Emiliano Fonda,<sup>§</sup> Alessandro Coati,<sup>#</sup> Yves Garreau,<sup>#,^</sup> Sara Bals,<sup>||</sup> Guy B. Marin,<sup>‡</sup> Christophe Detavernier,<sup>†</sup> and Jolien Dendooven<sup>\*,†</sup>

<sup>†</sup>Conformal Coating of Nanostructures (CoCooN), Department of Solid State Sciences, Ghent University, Krijgslaan 281 (S1), 9000 Ghent, Belgium

<sup>‡</sup>Laboratory for Chemical Technology, Ghent University, Technologiepark 125, B-9052 Zwijnaarde, Belgium

<sup>||</sup>Electron Microscopy for Materials Science (EMAT), University of Antwerp, Groenenborgerlaan 171, B-2020 Antwerp, Belgium

<sup>§</sup>SAMBA Beamline, <sup>#</sup>SixS Beamline, Synchrotron SOLEIL, L'Orme des Merisiers, Saint-Aubin, BP48, 91192 Gif-sur-Yvette, France, SOLEIL

<sup>^</sup>Université de Paris, Laboratoire Matériaux et Phénomènes Quantiques, CNRS, F-75013, Paris, France.

**Composition and thickness determination.** A series of pure Pt and In<sub>2</sub>O<sub>3</sub> films, with known thickness from XRR, were deposited and their specific weights calculated by assuming a bulk density. XRF measurements were then performed on these films and the respective fluorescence signal (Pt L $\alpha$  and In L $\alpha$ ) was integrated over a period of 100 s. A relationship obtained by plotting the XRF counts vs. the specific weight was used for determining the composition of the multilayer samples.

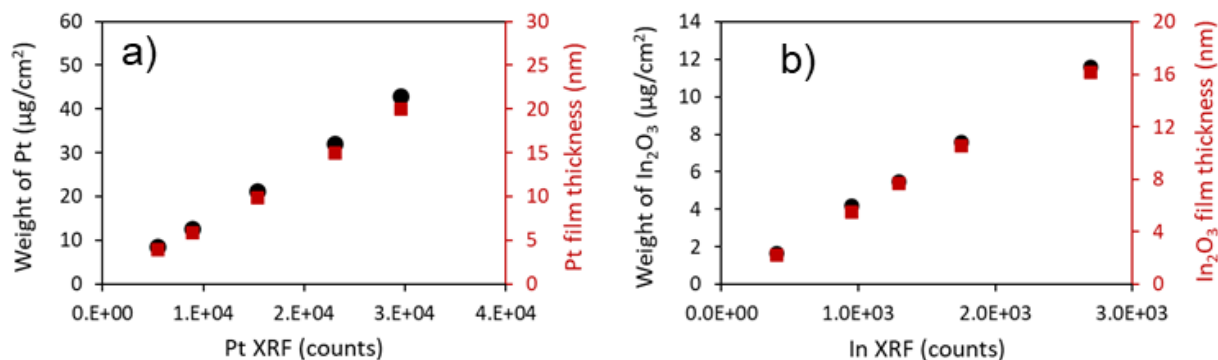


**Figure S1.** Variation of the specific weight (circles, left Y-axis) and thickness (squares, right Y-axis) of Pt (a) and In<sub>2</sub>O<sub>3</sub> (b) with the XRF intensity of Pt and In.

### Details of EXAFS analysis

Fourier transformation was performed from 2-3 Å<sup>-1</sup> as a lower boundary and 11-12 Å<sup>-1</sup> as the upper boundary, depending on the zero-point sectioning of the EXAFS k-space oscillation (**Figure S2**). This approach minimized the presence of so-called truncation ripples in the Fourier transformed EXAFS magnitude signal. The EXAFS fitting values of N, R and  $\sigma^2$  are summarized in the **table S1** and **S2**, in order to be able to better judge the estimated results. No pre-set values are used for the Debye-Waller disorder factors and the structural parameters were kept independent of each other to be able to compare the structural parameters for different samples in a sound way. To ensure that both were decoupled for each EXAFS fit, the binary correlation coefficients for the  $\sigma^2$  and N parameters was kept below 0.85.

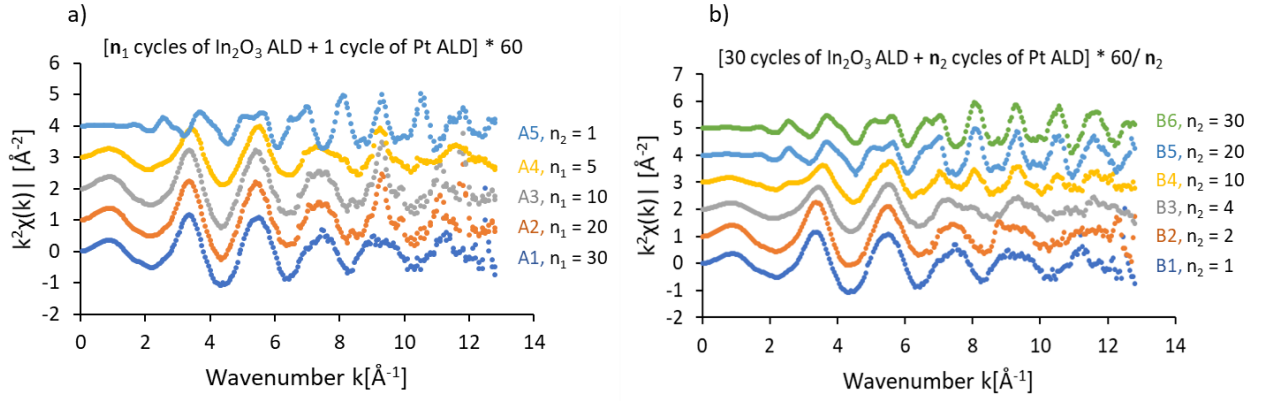


**Figure S2.** k-space EXAFS spectra of the samples in series A (a) and B (b).

**Table S1:** EXAFS fitting values for the samples in series A with ALD supercycles of [n<sub>1</sub> cycles of In<sub>2</sub>O<sub>3</sub> ALD + 1 cycle of Pt ALD] \* 60.

Sample	n <sub>1</sub>	N <sub>Pt-O</sub> [-]	R <sub>Pt-O</sub> [Å]	σ <sup>2</sup> <sub>Pt-O</sub> [10 <sup>-3</sup> Å <sup>2</sup> ]	N <sub>Pt-Pt</sub> [-]	R <sub>Pt-Pt</sub> [Å]	σ <sup>2</sup> <sub>Pt-Pt</sub> [10 <sup>-3</sup> Å <sup>2</sup> ]
A1	30	4.3±1.1	2.01±0.03	2.3±3.3	-	-	-
A2	20	4.2±0.5	2.01±0.01	0.3±1.3	-	-	-
A3	10	4.4±0.5	2.00±0.01	1.4±1.3	-	-	-
A4	5	3.0±0.3	2.01±0.01	0.7±1.3	1.1±0.3	2.78±0.02	0.7±1.3
A5	1	0.3±0.1	2.01±0.02	5.0±0.3	7.0±0.3	2.75±0.01	5.0±0.3

**Table S2:** EXAFS fitting values for the samples in series B with ALD supercycles of [30 cycles of In<sub>2</sub>O<sub>3</sub> ALD + n<sub>2</sub> cycle of Pt ALD] \* 60/n<sub>2</sub>.

Sample	n <sub>2</sub>	N <sub>Pt-O</sub> [-]	R <sub>Pt-O</sub> [Å]	σ <sup>2</sup> <sub>Pt-O</sub> [10 <sup>-3</sup> Å <sup>2</sup> ]	N <sub>Pt-Pt</sub> [-]	R <sub>Pt-Pt</sub> [Å]	σ <sup>2</sup> <sub>Pt-Pt</sub> [10 <sup>-3</sup> Å <sup>2</sup> ]
B1	1	4.3±1.1	2.01±0.03	2.3±3.3	-	-	-
B2	2	4.7±1.5	2.01±0.03	4.2±4.3	-	-	-
B3	4	3.4±0.5	2.00±0.02	3.6±2.0	1.2±1.4	2.74±0.03	4.8±8.2
B4	10	2.5±0.7	1.99±0.03	5.3±3.8	3.4±1.7	2.76±0.02	4.6±3.9
B5	20	0.3±0.1	1.95±0.02	5.5±0.3	7.5±0.3	2.76±0.002	5.5±0.3
B6	30	0.2±0.1	1.95±0.03	4.8±0.3	6.7±0.3	2.75±0.002	4.8±0.03

## GISAXS horizontal line profiles

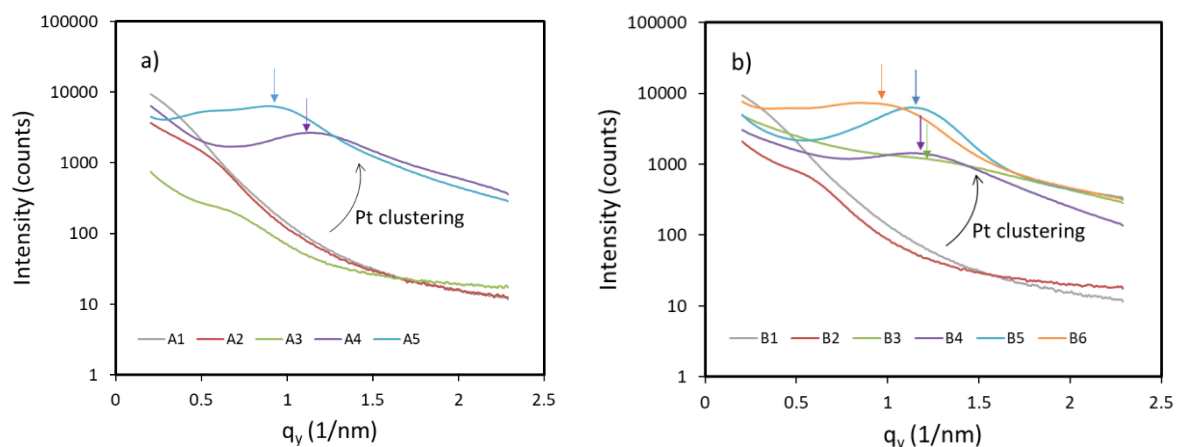


**Figure S3 (a, b)** Horizontal line profiles taken at the  $q_z$ -position of the main scattering maximum in the GISAXS patterns of the samples in series A and B, respectively.

**HR-STEM measurements.** Parts of samples B2 and B4 were cut and glued together facing each other. Cross-sectional samples suitable for STEM observations were prepared by an initial mechanical polishing, using an Allied Multiprep System with diamond-lapping films, down to a thickness of approximately 20  $\mu\text{m}$ , followed by  $\text{Ar}^+$  ion milling by using a Leica EM RES102 apparatus, with acceleration voltages up to 4 kV and incident beam angles between  $6^\circ$  and  $11^\circ$ . As visible in the overview STEM image (**Figure S4**), the thickness of both samples is uniform and found to be approximately 16.5 and 8.5 nm for samples B2 and B4, respectively, which is in close agreement with the thickness estimated using the XRF calibration.

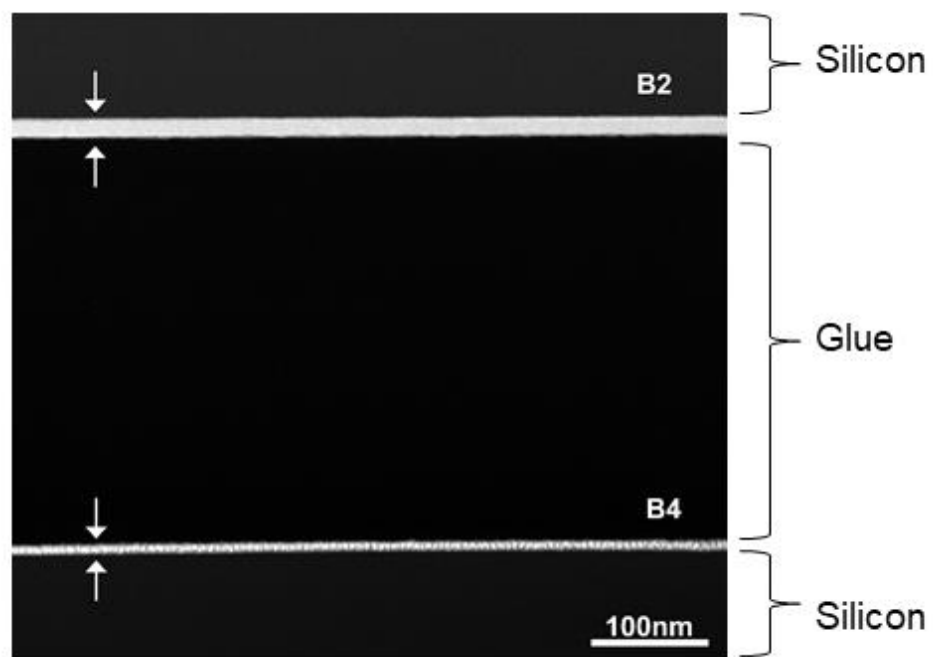


**Figure S4.** HAADF-STEM image showing the uniformity and thickness of sample B2 and B4.

Parts of samples B2 and B4 were glued facing each other and milled together.